The final publication is available at

https://doi.org/10.1002/jbm.a.35682

Additional Information

Influence of scaffold morphology on co-cultures of human endothelial and adipose tissue-derived stem cells

M. Arnal-Pastor[1, #], C. Martínez-Ramos[1, #], A. Vallés-Lluch[1], M. Monleón Pradas[1,2,*]

[1]*Center for Biomaterials and Tissue Engineering, Universitat Politècnica de València, C. de Vera s/n, 46022, Valencia, Spain*

[2]*Networking Research Center on Bioengineering, Biomaterials and Nanomedicine, Valencia, Spain*

*Corresponding author. Tel.: +34963877277; fax: +34963877276. E-mail: mmonleon@ter.upv.es

 # Equal contribution

Abstract

The interior of tissue engineering scaffolds must be vascularizable and allow adequate nutrients perfusion in order to ensure the viability of the cells colonizing them. The promotion of rapid vascularization of scaffolds is critical for thick artificial constructs. In the present study co-cultures of human endothelial and adipose tissue-derived stem cells have been performed in poly(ethyl acrylate) scaffolds with two different pore structures: grid-like (PEA-o) or sponge-like (PEA-s), in combination with a self-assembling peptide gel filling the pores, which aims to mimic the physiological niche. After 2 and 7 culture days, cell adhesion, proliferation and migration, the expression of cell surface markers like CD31 and CD90 and the release of VEGF were assessed by means of immunocytochemistry, scanning electronic microscopy, flow cytometry and ELISA analyses. The study demonstrated that PEA-s scaffolds promoted greater cell organization into tubular-like structures than PEA-o scaffolds, and this was enhanced by the presence of the peptide gel. Paracrine signaling from adipose cells significantly improved endothelial cell viability, proving the advantageous combination of this system for obtaining easily vascularizable tissue engineered grafts.

1. Introduction

Tissue engineering strategies combine cells with 3D-scaffolds that host them and improve their survival in the site of interest. Insufficient vascularization of thick scaffolds is considered to be one of the main causes for biohybrid grafts failure. For distances from the scaffold's surface greater than 100 microns, it is difficult to provide the necessary oxygen and nutrients supply as well as to remove waste products from the cells in the core of the scaffold.[1] Therefore, the vascularization of the scaffold's interior becomes a crucial factor to guarantee its success, and the onset of this process has frequently been studied *in vitro* with different cell types, either in monocultures or in co-cultures.[2]

Human adipose tissue-derived stem cells (hADSCs) are multipotent adult cells able to self-renew and differentiate into multiple lineages. Among their features, their relative ease of isolation and rapid expansion in culture outstands, which, together with their plasticity, make them excellent candidates for a wide variety of therapeutic applications.[3,4] Moreover, hADSCs can secrete a number of signals which might be helpful in the angiogenesis process.[5] A source of endothelial cells are the human umbilical vein endothelial cells (HUVECs), which have been used in many studies to obtain pre-vascularized scaffolds that could facilitate the regeneration of thick tissues.[6] These cells also release molecules that control cell proliferation and modulate vessel wall tone, and they have been used in works aiming at engineering new blood vessels and the regeneration of vascularized organs such as corneas[7], myocardium[8] or pancreas[9].

Previous works where hADSCs and HUVECs were co-cultured showed an increase of the capacity of endothelial cells to form a three-dimensional pre-vascular network and a much faster vascularization of the scaffold constructs *in vitro*, attributed to the presence of the hADSCs.[10,11,12] For this reason, these co-cultures were also chosen in the present study.

Cell features like morphology, differentiation capacity or cell-cell and cell-substrate adhesion are enhanced when cells are cultured in three-dimensional (3D) contexts. Such systems mimic better the *in vivo* microenvironment compared to traditional 2D culture ones.[13,14] Ideally, the scaffold used should be biocompatible in the implantation site, maintaining a 3D structure with interconnected pores that supports the migration and viability of cells along with the transport of nutrients, oxygen and wastes from the cells.[15,16] Among the many polymeric scaffolds used as 3D contexts[17,18], poly(ethyl acrylate) (PEA) with different porous structures has shown in previous studies very good biological properties *in vitro* with several cell types,[19,20,21,22,23,24] as well as *in vivo* in rats.[25]. The scaffold's pore structure provides a 3D environment at a scale much larger than cells size; it can thus be of interest to simultaneously attempt to simulate the cell's microenvironment at cell scale. For this purpose natural or synthetic peptide gels have been combined with scaffolds. The presence of the gel in the composite has been found to improve the biological performance of the systems.[26,27,28] In our study, the elastomeric PEA scaffolds were combined with the self-assembling peptide (SAP) gel RAD16-I as pores filling.[29,30]

Self-assembling peptide gels are a synthetic alternative to animal-derived extracellular matrix (ECM)-like materials. They present several advantages: there is no risk of illness transmission and all batches are homogeneous, *i.e.*, there is no variation in the amount of impurities, residual proteins or growth factors among batches.[31] The SAPs are commercialized in solution and under a change in their environment, like a pH modification or the addition of a salt,[32] are able to adopt beta-sheet structures and form a 3D network that mimics the natural ECM, with fibers in the range of 10-20 nm diameter and mesh sizes (pores) about 50-100 nm in diameter.[33] Among the wide variety of SAPs, RAD16-I is a multiple of the RADA aminoacid sequence. We have previously shown that the incorporation of RAD16-I in the scaffolds pores favors endothelial cell adhesion, survival, and migration *in vitro* and improves the uniformity of the seeded cells in them.[34,35]

PEA-based scaffolds presenting two different porous architectures (with orthogonal cylinders or with spherical interconnected pores) were combined in this work with the RADA16-I peptide gels. As regards vascularization of the scaffolds, the shape, size and connectivity of the pore structure can be of critical importance, since they define the overall geometrical constraints for the formation of tubular-like networks within the constructs. Co-cultures of hADSCs and HUVECs have thus been studied in both types of scaffolds, with and without RADA16-I gel to analyze the role of microarchitecture and gel filling. Cell distribution, formation of tubular-like structures, and VEGF (vascular endothelial growth factor) secretion have been followed as indicators of the performance of the combined biohybrid systems.

2. Materials and methods

2.1. Preparation of films

Films of poly(ethyl acrylate) were obtained by UV polymerization. Briefly, ethyl acrylate (EA; 99%, Sigma-Aldrich) with 2 wt% of ethylene glycol dimethyl acrylate (EGDMA; 98% Sigma-Aldrich) as crosslinker and 1 wt% of benzoin (Scharlab) as initiator were stirred for 15 min at room temperature. Then, the solution was injected between two glass plates separated by a wire of 1.2 mm in diameter, and placed in an ultraviolet oven for 8 h to let the polymerization occur. Subsequent post-polymerization was carried out at 90ºC for 24 h. At that moment films were rinsed for 24 h in boiling ethanol, which was changed every 8 h, to remove residues. Finally, films were dried at room conditions for 24 h, 24 h more under vacuum and under vacuum at 60ºC for 24 extra hours before any ensuing experiment.

2.2. Preparation of scaffolds with cylindrical pores morphology

PEA scaffolds with orthogonally arranged cylindrical pores (PEA-o hereafter) were obtained with a nylon porogen template previously prepared, following the procedure described in[36]. Concisely, eight layers of nylon fabrics (SAATI S.A., Barcelona, Spain) with nominal thread diameter equal to 150 μm and mesh opening of 300 μm were stacked and sintered under pressure and temperature. The porogen template was placed between glass plates and a mixture of EA monomer with 0.1 wt% of azo-bis-isobutyronitrile (99%, Fluka), AZBN, as thermal initiator, and 2 wt% of EGDMA as crosslinker was injected in it and polymerized for 24 h at 60ºC. Next, a 24 h post-polymerization step at 90ºC was

carried out. The materials were rinsed in 30% nitric acid aqueous solution (60%, Scharlab), repeatedly changed during 4 days, to dissolve the nylon template. Then, scaffolds were rinsed in boiling water for 16 h (the water was changed every 8 hours) to remove nitric acid traces. Scaffolds were dried following the same steps as for films before use.

2.3. Preparation of scaffolds with spherical pores morphology

PEA scaffolds with isotropically intersecting spherical pores (PEA-s hereafter) were obtained by using a poly(methyl methacrylate), PMMA, template obtained by sintering microspheres (Colacryl dp 300) under pressure and temperature, following the procedure described in[37]. These templates were also placed between glass plates and then, the EA monomeric solution with 2 wt% EGDMA and 1 wt% benzoin was injected and polymerized with UV light for 24 h and finally post-polymerized for 24 extra hours at 90ºC. The PMMA template was eliminated by solution in acetone in a soxhlet extractor. Once the PMMA was completely removed, acetone was progressively exchanged with water and then the scaffolds were dried following the same steps as films and PEA-o scaffolds. All materials were sterilized in an autoclave at 121ºC and under pressure prior to their use in cell culture experiments.

2.4. Loading of the self-assembling peptide solution in the scaffolds' pores

An analogous procedure to that presented in [29] was followed. Briefly, 5 mm diameter scaffolds were placed in a syringe and then distilled water was loaded; the luer tape of the syringe was sealed and 5 strokes of the plunger of 4 mL each were applied to ensure the penetration of water inside the scaffolds' pores. Next, the self-assembling peptide solution (Puramatrix, BD Biosciences) diluted

at 0.3% w/v in ultradeionized water following a 30 min sonication, was loaded in the syringe and again four strokes of the plunger were applied.

2.5. Co-culture of HUVECs and hADSCs

HUVECs (Gibco) were cultured in flasks with Medium 200 (Invitrogen) supplemented with LSGS (Low serum growth supplement, Invitrogen), 0.1% gentamicin (Gibco), 100 U ml^{-1} penicillin and 100 µg ml^{-1} streptomycin until 80% confluence was reached. Then, cells were trypsinized, collected and centrifuged at 180 g for 7 minutes.

Human mesenchymal stem cells derived from adipose tissue from a commercial cell line (HC016, Histocell, Spain) in their 6th passage were cultured until confluence with Ham's F-12 nutrients mixture with 1% L-glutamine (Life technologies), 10% (v/v) fetal bovine serum (FBS), and 100 U ml^{-1} penicillin, 100 µg ml^{-1} streptomycin. Next, cells were trypsinized, collected and centrifuged at 1000 rpm for 5 min.

hADSCs and HUVECs were counted and combined in a 1 to 3 proportion. Bare and SAP-filled scaffolds (both PEA-o and PEA-s) samples, 5 mm in diameter, were seeded with 4 x 10^5 cells in 20 µL drops of the medium described below. The drop was placed on the top surface of PEA-o scaffolds with a micropipette and injected in the center of PEA-s scaffolds with a Hamilton syringe, because the latter are less porous and cell migration would otherwise be hindered. Seeded scaffolds were kept 30 min in a Titramax 101 shaker (Heidolph instruments, Germany) inside the incubator and afterwards the medium was completed. Bulk materials used as controls were analogously cultured but with 4 x 10^4 cells in 10 µL drops, which is a lower density than that used in scaffolds,

because films present less surface available for the cells to adhere. The co-culture medium was a 1 to 3 mixture of hADSCSs and HUVECs culture media. It was renewed every day up to 10 days.

2.6. Flow cytometry

Flow cytometry scans were performed to evaluate the evolution of each cell subpopulation with time. To do this, at each selected time points (2 and 7 days), cells in 5 replicates per group were trypsinized, pooled, and subsequently blocked for 30 min with BSA 1% in DPBS. As suggested by the supplier, a minimum of 1×10^6 cells per group were incubated in a 100-µl test sample for 30 min at 4°C with FITC mouse anti-human CD31 (1:5, BD Bioscience, 560984) and APC mouse anti-human CD90 (1:20, BD Bioscience, 561971) diluted in PBSA. Finally, cells were rinsed twice, re-suspended with DPBS and scanned in a High Speed Cell Sorter MoFlo flow cytometer (Beckman-Coulter, CA, USA). 1:300 propidium iodide (1 mg/mL in water, Sigma-Aldrich) was added to the cell suspension to discard dead cells from the analyses.

2.7. Quantitative DNA analysis

Cell density was also estimated by means of a Quant-iT™ PicoGreen® dsDNA Assay Kit (Invitrogen). Briefly, after 7 days, samples were washed with PBS and frozen in a -80ºC freezer. Once thawed, samples were digested with Proteinase K (Roche) diluted 1 to 20 in DPBS at pH 8.1 for 16 h under gently shaking; next, the enzyme was inactivated for 10 min at 90ºC. As soon as they were tempered, the samples were vortexed for 1 min and centrifuged for 1 min at 650 g. Next, 28.7 µL of the supernatants and standards were mixed with 28.52 µL of

the Picogreen reagent at a 1:200 concentration in Tris-EDTA (TE) buffer, and 100 µL more of TE buffer was added to each well in a 96-well plate. After 5 min of incubation, fluorescence was measured in a Victor Multilabel Counter 1420 spectrophotometer (Perkin Elmer, Waltham, MA, USA) at 535 nm.

2.8. Morphological characterization of cultured materials by SEM

Cell morphology after culture in the different materials was observed by scanning electron microscopy (SEM). At the selected times, cultured samples were fixed by immersion in 2.5% glutaraldehyde (Electron Microscopy Science) in 0.1 M phosphate buffer (PB) for 1 h at 37ºC. Next, samples were post-fixed with osmium tetroxide (Electron Microscopy Science) for 1 h, rinsed three times with distilled water, and dehydrated by immersing them in aqueous solutions with increasing ethanol fractions (30%, 50%, 70%, 96%, and 100% of ethanol). Once dehydrated, the samples were critical-point dried with an Autosambri 814 instrument (Rockville, MD, USA) and sputter-coated with gold before observation under a Hitachi S-4800 microscope at 10 kV.

2.9. Immunocytochemistry

The lay-out of endothelial cells in PEA-o and PEA-s scaffolds was identified via endothelial-cell specific PECAM1 (CD31) immunostaining. At the selected time points, samples were gently rinsed with DPBS twice and fixed with a 4% paraformaldehyde (PFA; Panreac) solution at room temperature. After 10 min the solution was removed and the samples were rinsed with DPBS three times. Next, samples were incubated at room temperature with blocking and permeabilizing buffer (BPB) for 1 h. BPB was composed of DPBS (Sigma-

Aldrich), 10% FBS and 1% triton X-100 (Sigma-Aldrich). Finally, two 5 min DPBS rinses were performed.

Once blocked and permeabilized, samples were incubated overnight, in the dark at 4°C in a solution of BPB containing mouse monoclonal antibody against CD31 (1:100; Chemicon). Then, samples were rinsed with DPBS for 5 min three times. Next, the secondary antibody, goat anti-mouse Alexa 647 (1:200; Invitrogen) was added and incubated for 1 h at room temperature, followed by a 5 min wash with DPBS. Finally, samples were stained with 1:5000 4′,6-diamidino-2-phenylindole dihydrochloride (DAPI; Sigma)/H_2O solution for 10 min, followed by two DPBS rinses. After the staining protocol, samples were mounted with Fluorsave reagent (Merck Millipore), coverslipped and examined with a Nikon eclipse 80i fluorescence microscope or a confocal laser scanning microscope (LSM, Zeiss 780 Axio observer z1).

In order to observe the inner cross-sections of the cultured scaffolds, they were rinsed twice with PBS after the staining protocols, cryopreserved in 30% sucrose, embedded in frozen section compound (Leica) and cut into 100 μm slices.

2.10. Quantification of VEGF release

The accumulated VEGF (vascular endothelial growth factor) release by cells to the culture medium along the co-culture experiment was quantified by means of a human VEGF Enzyme-Linked ImmunoSorbent Assay (ELISA, R&D systems, DY293B). Medium supernatant was collected every two days, and next the kit was used following manufacturer's instructions.

2.11. Statistical analysis

The results are expressed as mean ± standard deviation from at least three replicates. Data were analyzed pair wise with ANOVA test with Statgraphics Centurion XVI.I. Statistically significant differences are noted in the results with an * for a p-value < 0.05.

3. Results

3.1 Characterization of the scaffolds morphologies

The two types of scaffolds prepared present very different pore morphologies: PEA-s scaffolds have a pore structure consisting in isotropically intersecting spherical (sponge-like) pores of around 90 microns in diameter (Figure 1 A and B), whereas the pores of the PEA-o scaffolds consist in orthogonally intersecting arrays of cylindrical channels (grid-like) with a diameter of the order of 150 microns (Figure 1 C and D). PEA-s scaffolds have a pore volume fraction of 80.8 ± 3.5%[26], whereas that of PEA-o scaffolds is 76.4±6.1%.[35]

3.2 Study of cell markers in co-cultures in the systems

We assessed the biological performance of both types of scaffolds (PEA-s and PEA-o) in combination with self-assembling peptide gel when seeded simultaneously with HUVECs and hADSCs. Flow cytometry was used to evaluate the fraction of each type of cells present in the scaffolds, and its evolution with time. As observed in Figure 2, the fraction of endothelial, CD31– positive cells in PEA-o scaffolds at short times is higher in bare scaffolds than in those filled with the SAP gel; at longer times, the fraction of CD31+ cells decreases in bare scaffolds, while it increases in the scaffolds with SAP gel

(Figure 2A). On the contrary, the fraction of mesenchymal CD90+ cells increases with time in bare PEA-o scaffolds, while that fraction remains constant in the SAP-filled ones (Figure 2B).

Different results were obtained with PEA-s scaffolds (Figure 3). Both bare scaffolds and those combined with the SAP gel showed a significant decrease of HUVECs fraction with culture time, while the fraction of mesenchymal cells increased significantly.

3.3 Cell density, distribution and morphology

Cell density was evaluated for each group of materials by quantifying the DNA content through a picoGreen assay. Figure 4 shows that similar values were obtained for the different groups, regardless of the type of porous structure and the presence or absence of SAP (except for the PEA-o/SAP system, with a somewhat lower DNA content).

Cell distributions throughout the scaffolds were studied by SEM. In PEA-o samples, either bare or with the SAP gel, a great number of cells was observed, which coated the scaffold's external surface (Figure 5A,C) and were uniformly distributed throughout the cross-sections (Figure 5B,D). In bare PEA-o scaffolds cells adopted elongated shapes following the cylindrical pores; in PEA-o/SAP scaffolds, more rounded structures were found. The SEM images do not allow to distinguish cells from their ECM and the peptide gel. In PEA-s scaffolds cells also coated uniformly the external surface (Figure 6 A,C), the cell layer being denser in the SAP-filled ones. When cross sections were exposed, a high density of cells was detected in bare scaffolds (Figure 6 B,D).

The lay-out of HUVECs was further assessed by CLSM after 10 days of co-culture through immunostaining of CD31 (Figures 7-9). Cells cultured in bare PEA-o scaffolds (Figure 7A,B) laid extended along the channels and adhered to the pore surfaces and edges, while cells cultured in the PEA-o/SAP system tended to form clusters and to establish connections between them, suspended in the gel within the pores (Figure 7 C,D). Analogous surface images of the PEA-s scaffolds (Figure 8 A,C) show a great cell density in both bare and SAP-filled systems. Immunostaining of CD31 showed abundant protocapillary-like structures in PEA-s at day 10, as HUVECs organized into extensive branched and network-like arrangements. In SAP-filled PEA-s systems cells seemed to follow a more organized distribution (asterisks in Figure 8C), where circle-like cell dispositions are observed, while in bare systems cell distribution seems more chaotic. In the cross–sections of PEA-s/SAP scaffolds more complex assemblies of cells were observed (Figure 8 D), forming circular 3D structures that might be precursors of a tubular structure.

Views at low magnification of the inner cross-sections of both types of scaffolds obtained by reconstruction from sets of 16 CLSM images were used to study the overall uniformity of cell distribution (Figure 9). In PEA-s scaffolds, either bare or filled with the gel, cells are evenly distributed throughout their thickness, establishing contacts between them, many of them adopting a circular disposition (highlighted with asterisks in Figure 9 C,D), while in PEA-o scaffolds cells are more uniformly distributed if bare, and form occasional aggregates if filled with the gel (Figure 9 A,B).

3.4 Release of VEGF

The release of VEGF to the medium by cells cultured in the different materials (Figure 10) did not show differences between PEA-s scaffolds with pores filled or not with the SAP gel. In PEA-o systems, however, a slightly greater release was observed when bare. A comparison of both scaffold typologies shows that cells cultured in PEA-s scaffolds released more VEGF (up to 10 times more) than those cultured in PEA-o ones (either bare or filled with gel). Remarkably, VEGF-release from cells cultured within all types of scaffolds was much greater than the amount released from cultures on flat substrates (coverslips).

4. Discussion

The two scaffold types of our study have the same material chemistry, but differ in the morphology of their pore architecture. PEA-o scaffolds have a smaller pore volume fraction and larger inner neat continuous surfaces available for cell adhesion. Furthermore, pores in the PEA-o structure are long cylinders, interconnected only at separations corresponding to the contact points of the porogenic fabric layers (Figures 1 and 5). By contrast, PEA-s scaffolds have a larger pore volume fraction and their pores are spherical cavities with a high coordination number, and thus the neat interior surfaces available for cell adhesion have much smaller area and are in the form of thin struts defined by the interspaces left by the original porogenic template of sintered beads. Thus, PEA-o scaffolds have a highly anisotropic porous structure, with low interconnectivity and large interior surfaces, whereas PEA-s scaffolds have an nearly isotropic porous structure with high interconnectivity and less internal

surface available. These geometrical differences influence the dissimilar colonization patterns of HUVECs and hADSCs in the scaffolds. hADSCs are larger than HUVECs, and more proliferative.[17] All studied scaffold structures were seeded with the same cell number, in a HUVECs:hADSC proportion of 3:1, and after 7 days no significant differences in the total cell density were detectable (Figure 4). However, the ratio of endothelial to mesenchymal cells had changed: at day 2 it was much higher than initially, and diminished with time along the experiment (Figs 2, 3), except in the case of PEA-o/SAP scaffolds. Since hADSCs are much larger than HUVECs, some of the initially seeded hADSCs may not have reached the interior of the scaffolds; those who did, proliferated at a faster rate than HUVECs, and thus the ratio was reversed in due time. Many HUVECs in the PEA-s systems establish cell-cell contacts (Figure 8), which leads to a lower proliferation due to inhibition by contact, as discussed in[38]. The low magnification reconstruction of bare and SAP-filled PEA-s scaffolds (Figure 9) reveals that cells were capable of migrating through the scaffolds pores. Due to the larger exposed surfaces of PEA-o scaffolds, many more cells were lost when samples were processed for observation than from PEA-s ones.

A significant challenge in tissue engineering is to induce the rapid vascularization of scaffolds to ensure the survival of transplanted and invader cells. Vascular endothelial growth factor (VEGF) is one of the most effective growth factors to promote the formation of new blood vessels and induces a large number of biological responses on endothelial cells.[39,40,41]This growth factor is secreted by several cell types, hADSCs among them.[42,43,44] Thus,

besides other reported paracryne effects, transplantation of hADSCs can be useful in achieving a fast vascularization of the implant. In our systems, a great difference in the concentration of secreted VEGF was observed depending on the materials where cells were co-cultured (Figure 10). Cultures on planar 2D materials expressed the lowest amounts of VEGF, in good agreement with other works.[45] The large difference of VEGF release between PEA-o and PEA-s scaffolds is remarkable, but consistent with the fact that VEGF is secreted by hADSCs,[46] which at day 7 are more abundant in PEA-s systems than in PEA-o ones (Figure 10). Furthermore, PEA-s scaffolds seem to provide an environment where the formation of HUVECs networks through cell-to-cell contacts is more favorable: these structures were detected in PEA-s systems, but not in PEA-o ones (Figures 7-9). The open-pore morphology of PEA-s scaffolds thus seems to allow more freedom for cell organization than does the much more constraining pore architecture of PEA-o ones. These positive results with PEA-s scaffolds are even better when the peptide gel is incorporated in the pores (Figure 9). The gel-like environment thus seems to further enhance the mobility of the seeded cells needed for their spatial rearrangement.

5. Conclusions

Co-cultures of HUVECs and hADSCs can be maintained in PEA-o and PEA-s scaffolds with SAP gel in their pores. HADSCs secrete in the scaffold systems much more VEGF than in cultures on planar structures. The wider pores and larger pore interconnectivity of PEA-s scaffolds provide the necessary freedom for HUVECs to reorganize and form branched cell networks throughout them.The peptide gel enhances these effects. These results suggest that the

17

pore architecture of sponge-like scaffolds has a greater vascularization potential than that of grid-like ones.

Acknowledgements

References

[1]Jain RK, Au P, Tam J,. Duda DG, Fukumura D. Engineering vascularized tissue. Nat Biotechnol 2005;23:821-3.

[2]Kirkpatrick CJ, Fuchs S, Unger RE. Co-culture systems for vascularization-learning from nature. Adv Drug Deliv Rev 2011; 63:291-9.

[3]Katsuda T, Kurata H, Tamai R, Banas A, Ishii T, Ishikawa S, Ochiya T. The in vivo evaluation of the therapeutic potential of human adipose tissue-derived mesenchymal stem cells for acute liver disease. Methods Mol Biol 2014;1213:57-67.

[4]Lewis CM, Suzuki M. Therapeutic applications of mesenchymal stem cells for amyotrophic lateral sclerosis. Stem Cell Res Ther 2014;5(2):32.

[5]Deveza L, Choi J, Imanbayev G, Yang F. Paracrine release from nonviral engineered adipose-derived stem cells promotes endothelial cell survival and migration in vitro. Stem Cells Dev 2013;22:483-91.

[6]Kaully T, Kaufman-Francis K, Lesman A, Levenberg S. Vascularization-the conduit to viable engineered tissues. Tissue Eng Part B Rev 2009;15:159-69.

[7]Nishida K, Yamato M, Hayashida Y, Watanabe K, Maeda N, et al. Functional bioengineered corneal epithelial sheet grafts from corneal stem cells expanded ex vivo on a temperature-responsive cell culture surface. Transplantation 2004;77:379-85.

[8]Sekine H, Shimizu T, Yang J, Kobayashi E, Okano T. Pulsatile myocardial tubes fabricated with cell sheet engineering. Circulation 2006;114:I87-93.

[9]Shimizu H, Ohashi K, Utoh R, Ise K, Gotoh M, Yamato M, Okano T. Bioengineering of a functional sheet of islet cells for the treatment of diabetes mellitus. Biomaterials 2009;30:5943-9.

[10]Sánchez-Muñoz I, Granados R, Holguín Holgado P, García-Vela JA, Casares C, Casares M. The Use of Adipose Mesenchymal Stem Cells and Human Umbilical Vascular Endothelial Cells on a Fibrin Matrix for Endothelialized Skin Substitute. Tissue Eng Part A 2015;21(1-2):214-23.

[11]Kim KI, Park S, Im GI. Osteogenic differentiation and angiogenesis with co-cultured adipose-derived stromal cells and bone marrow stromal cells. Biomaterials 2014;35:4792-804.

[12]Strassburg S, Nienhueser H, Björn Stark G, Finkenzeller G, Torio-Padron N. Co-culture of adipose-derived stem cells and endothelial cells in fibrin induces angiogenesis and vasculogenesis in a chorioallantoic membrane model. J Tissue Eng Regen Med 2013 May 27, in press.

[13]Pampaloni F, Reynaud EG, Stelzer EH. The third dimension bridges the gap between cell culture and live tissue. Nat Rev Mol Cell Biol 2007;8: 839-845.

[14]Santos E, Hernández RM, Pedraz JL, Orive G. Novel advances in the design of three-dimensional bio-scaffolds to control cell fate: translation from 2D to 3D. Trends Biotechnol 2012;30:331-41.

[15]Artel A, Mehdizadeh H, Chiu YC, Brey EM, Cinar A. An agent-based model for the investigation of neovascularization within porous scaffolds. Tissue Eng Part A 2011;17:2133-41.

[16]Choi SW, Zhang Y, Macewan MR, Xia Y. Neovascularization in biodegradable inverse opal scaffolds with uniform and precisely controlled pore sizes. Adv Healthc Mater 2013;2:145-54.

[17]Bidarra SJ, Barrias CC, Barbosa MA, Soares R, Amédée J, Granja PL. Phenotypic and proliferative modulation of human mesenchymal stem cells via crosstalk with endothelial cells. Stem Cell Res 2011;7:186-97.

[18]Skiles ML, Hanna B, Rucker L, Tipton A, Brougham-Cook A, Blanchette JO. ASC spheroid geometry and culture oxygenation differentially impact induction of pre-angiogenic behaviors in endothelial cells. Cell Transplant 2014 Aug 21, in press.

[19]Rico P, Rodríguez Hernández JC, Moratal D, Monleón Pradas M, Salmerón Sánchez M. Substrate-induced assembly of fibronectin into networks. Influence of surface chemistry and effect on osteoblast adhesion. Tissue Eng 2009;15:3271-3281.

[20]Soria JM, Sancho-Tello M, García Esparza MA, Mirabet V, Bagan JV, Monleón Pradas M, Cardá C. Biomaterials coated by dental pulp cells as substrate for neural stem cell differentiation. J Biomed Mater Res Part A 2011;97:85-92.

[21]Soria JM, Martínez-Ramos C, Salmerón-Sánchez M, Benavent V, Campillo-Fernández A, Gómez-Ribelles JL, García Verdugo JM, Monleón Pradas M. Survival and differentiation of embryonic neural explants onto different biomaterials. J Biomed Mater Res Part A 2006;79:495-502.

[22]Campillo-Fernández AJ, Pastor S, Abad-Collado M, Bataille L, Gómez Ribelles JL et al. Future design of a new keratoprosthesis. Physical and biological analysis of polymeric substrates for epithelial cell growth. Biomacromolecules 2007;8:2429-2436.

[23]Pérez Olmedilla M, García-Giralt N, Monleón Pradas M, Benito Ruiz P, Gómez Ribelles JL et al. Response of human chondrocytes to a non-uniform distribution of hydrophilic domains on poly(ethyl acrylate-co-hydroxyethyl methacrylate) copolymers. Biomaterials 2006;27:1003-1012.

[24]Ying M, Saha K, Bogatyrev S, Yang J, Hook AL et al. Combinatorial development of biomaterials for clonal growth of human pluripotent stem cells. Nature Materials 2010;9:768-778.

[25]Martínez-Ramos C, Vallés-Lluch A, García Verdugo JM, Gómez Ribelles JL, Barcia Albacar JA et al. Channeled scaffolds implanted in adult rat brain. J Biomed Mater Res A 2012;100:3276-3286.

[26]Wang X, Li Q, Hu X, Ma L, You C et al. Fabrication and characterization of poly(L-lactide-co-glycolide) knitted mesh-reinforced collagen-chitosan hybrid scaffolds for dermal tissue engineering. J Mech Behav Biomed Mater 2012;8: 204-15.

[27]Godier-Furnémont AFG, Martens TP, Koeckert MS, Wan L, Parks J et al. Composite scaffold provides a cell delivery platform for cardiovascular repair. PNAS 2011;108(19): 7974–7979.

[28]Chen K, Sahoo S, He P, Ng KS, Toh SL, Goh JC. A hybrid silk/RADA-based fibrous scaffold with triple hierarchy for ligament regeneration. Tissue Eng Part A 2012;18(13-14):1399-409.

[29]Vallés-Lluch A, Arnal-Pastor M, Martínez-Ramos C, Vilariño-Feltrer G, Vikingsson L et al. Combining self-assembling peptide gels with three-dimensional elastomer scaffolds. Acta Biomaterialia 2013;9:9451-9460.

[30]Martínez-Ramos C, Rodríguez-Pérez E, Pérez Garnes M, Chachques JC, Moratal D et al. Design and Assembly Procedures for Large-Sized Biohybrid Scaffolds as Patches for Myocardial Infarct. Tissue Eng Part C Methods 2014;20:817-27.

[31]Zhang S, Gelain F, Zhao X. Designer self-assembling peptide nanofiber scaffolds for 3D tissue cell cultures. Semin Cancer Biol 2005;15:413-20.

[32]Davis ME, Motion JP, Narmoneva DA, Takahashi T, Hakuno D et al. Injectable self-assembling peptide nanofibers create intramyocardial microenvironments for endothelial cells. Circulation 2005;111(4):442-50.

[33]Zhang S, Altman M. Peptide self-assembly in functional polymer science and engineering. Reactive & Functional Polymers 1999;41:91-102.

[34]Martínez-Ramos C, Arnal-Pastor M, Vallés-Lluch A, Monleón Pradas M. Peptide gel in a scaffold as a composite matrix for endothelial cells. J Biomed Mater Res A 2015 Mar 23, in press.

[35] Vallés-Lluch A, Arnal-Pastor M, Martínez-Ramos C, Vilariño-Feltrer G, Vikingsson L, Monleón Pradas M. Grid polymeric scaffolds with polypeptide gel filling as patches for infarcted tissue regeneration. Conf Proc IEEE Eng Med Biol Soc 2013:6961-4.

[36]Rodríguez Hernández JC, Serrano Aroca A, Gómez Ribelles JL, Monleón Pradas M. Three-dimensional nanocomposite scaffolds with ordered cylindrical orthogonal pores. J Biomed Mater Res B Appl Biomater 2008;84: 541-9.

[37]Diego RB, Olmedilla MP, Aroca AS, Gómez Ribelles JL, Monleón Pradas M et al. Salmerón Sánchez. Acrylic scaffolds with interconnected spherical pores and controlled hydrophilicity for tissue engineering. J Mater Sci Mater Med 2005;16: 693-8.

[38]Twardowski RL, Black III LD. Cardiac Fibroblasts Support Endothelial Cell Proliferation and Sprout Formation but not the Development of Multicellular Sprouts in a Fibrin Gel Co-Culture Model. Ann Biomed Eng 2014;42:1074-84.

[39]Carmeliet P, Jain RK. Molecular mechanisms and clinical applications of angiogenesis. Nature 2011;473:298-307.

[40]Eichmann A, Simons M. VEGF signaling inside vascular endothelial cells and beyond. Curr Opin Cell Biol 2012;24:188-193.

[41]Phelps EA, Garcia AJ. Update on therapeutic vascularization strategies. Regen Med 2009;4:65-80.

[42]Deveza L, Choi J, Imanbayev G, Yang F. Paracrine release from nonviral engineered adipose-derived stem cells promotes endothelial cell survival and migration in vitro. Stem Cells Dev 2013;22:483-91.

[43]Iyyanki TS, Dunne LW, Zhang Q, Hubenak J, Turza KC, Butler CE. Adipose-Derived Stem-Cell-Seeded Non-Cross-Linked Porcine Acellular Dermal Matrix Increases Cellular Infiltration, Vascular Infiltration, and Mechanical Strength of Ventral Hernia Repairs. Tissue Eng Part A 2015;21(3-4):475-85.

[44]Rohringer S, Hofbauer P, Schneider KH, Husa AM, Feichtinger G et al. Mechanisms of vasculogenesis in 3D fibrin matrices mediated by the interaction of adipose-derived stem cells and endothelial cells. Angiogenesis 2014;17:921-33.

[45]Neofytou EA, Chang E, Patlola B, Joubert LM, Rajadas J et al. Adipose tissue-derived stem cells display a proangiogenic phenotype on 3D scaffolds. J Biomed Mater Res A 2011;98:383-93.

[46]Beckermann BM, Kallifatidis G, Groth A, Frommhold D, Apel A et al. VEGF expression by mesenchymal stem cells contributes to angiogenesis in pancreatic carcinoma. Br J Cancer 2008;99:622-31.

Figure legends
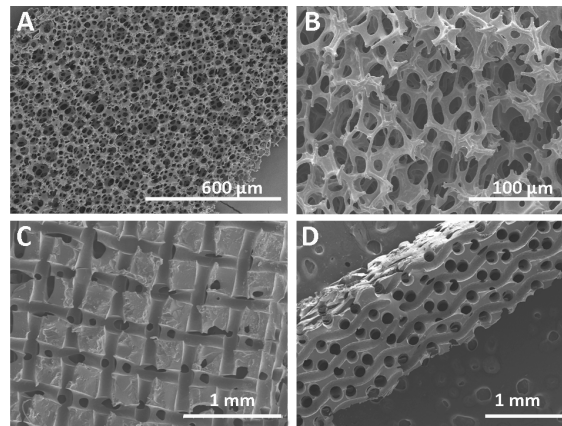
Figure 1: Scanning electron micrographies of PEA-s (A and B) and PEA-o scaffolds (C and D).
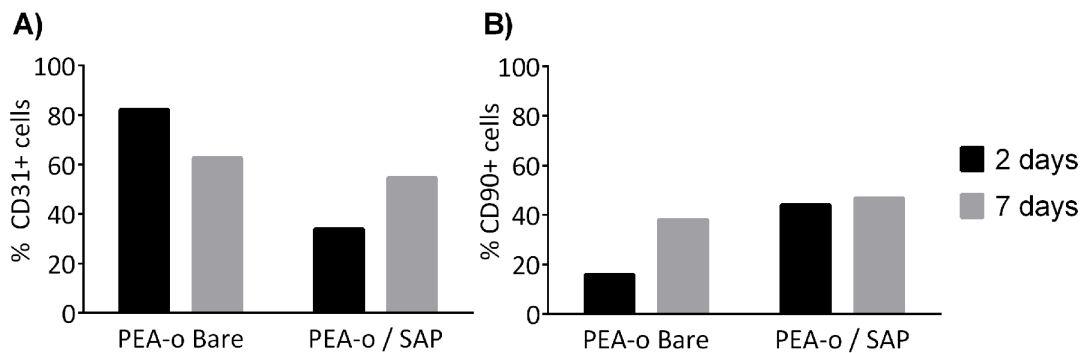

Figure 2: Fractions (%) of CD31 (A) and of CD90 (B) positive cells in the bare and SAP-filled PEA-o scaffolds after 2 and 7 days of culture.
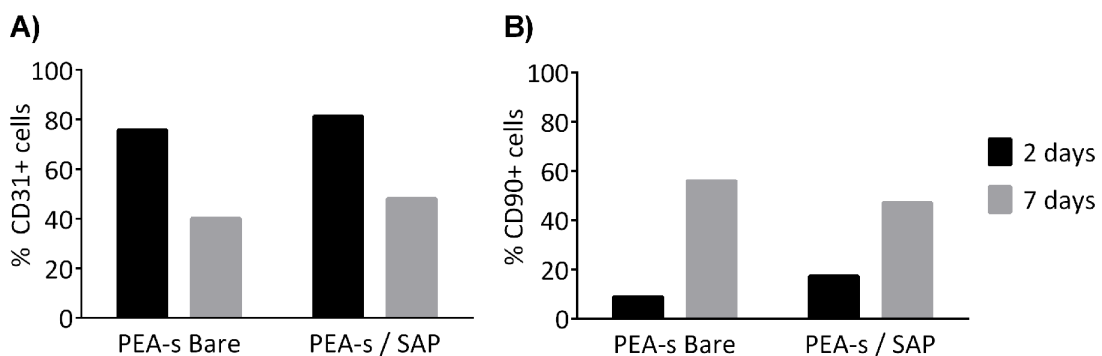

Figure 3: Fractions (%) of CD31 (A) and of CD90 (B) positive cells in the bare and SAP-filled PEA-s scaffolds after 2 and 7 days of culture.
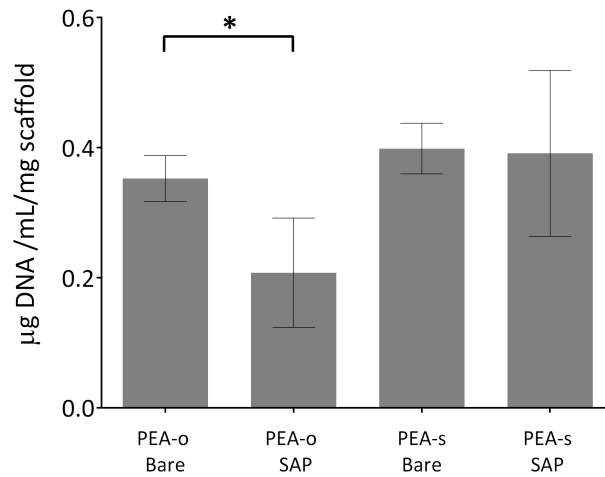
Figure 4: DNA content in the different types of scaffolds after 7 days of culture. (*) Statistically significant differences, p-value< 0.05.
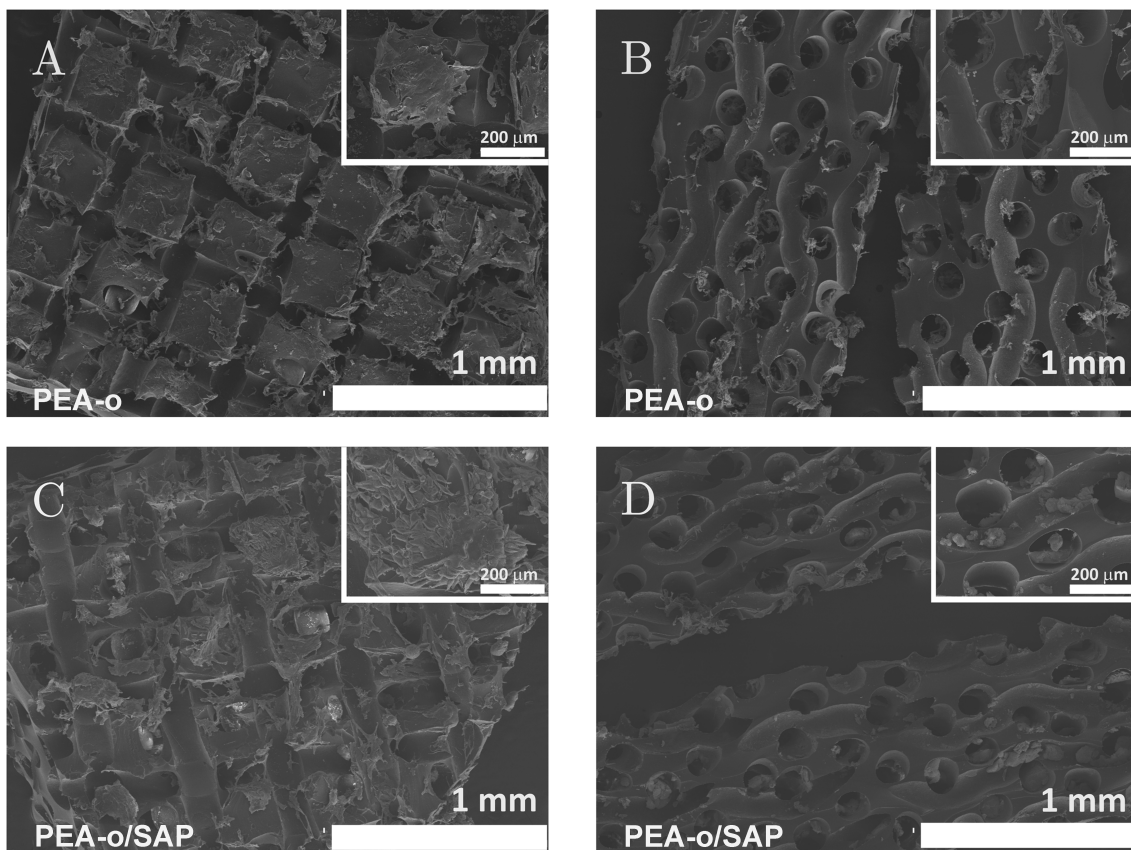
Figure 5: SEM images of the surfaces (A, C) and cross-sections (B, D) of PEA-o scaffolds without (A, B) and with SAP gel in the pores (C, D), seeded dynamically with HUVECs and hADSCs, after 10 days of culture. Insets show details of regions of interest at greater magnifications.
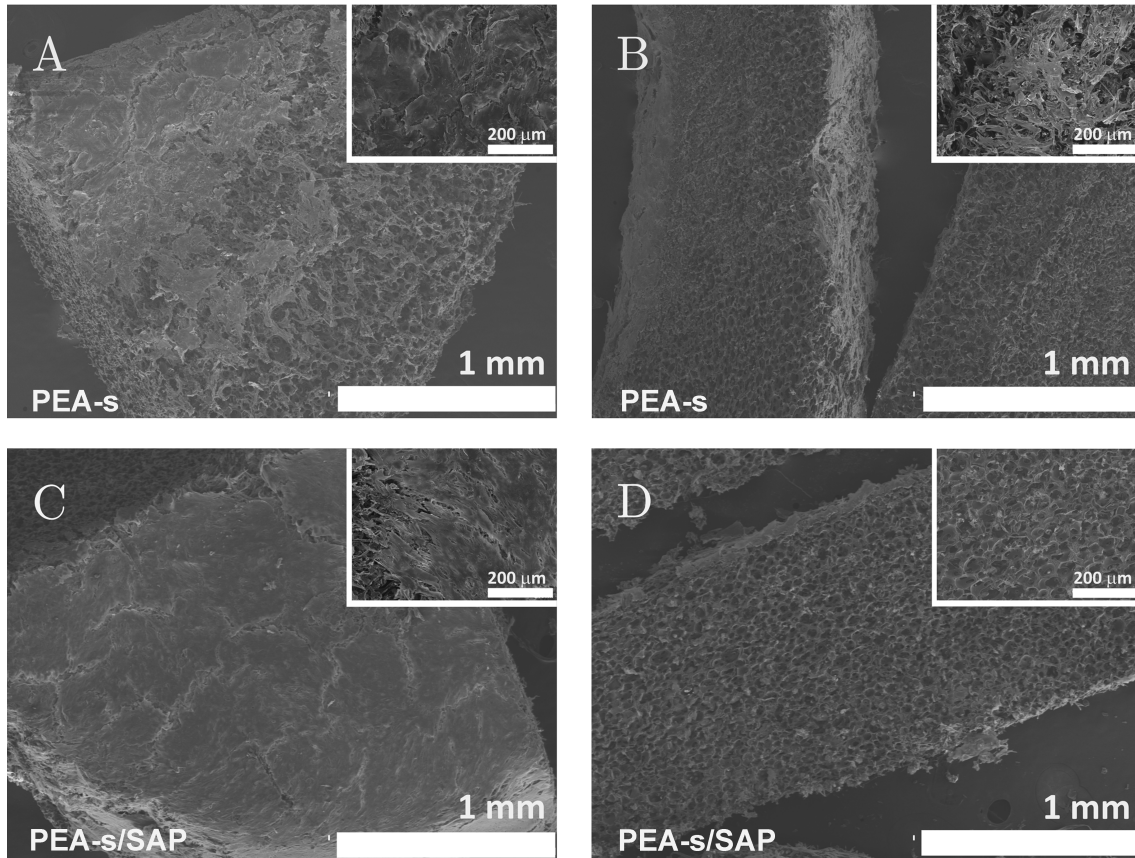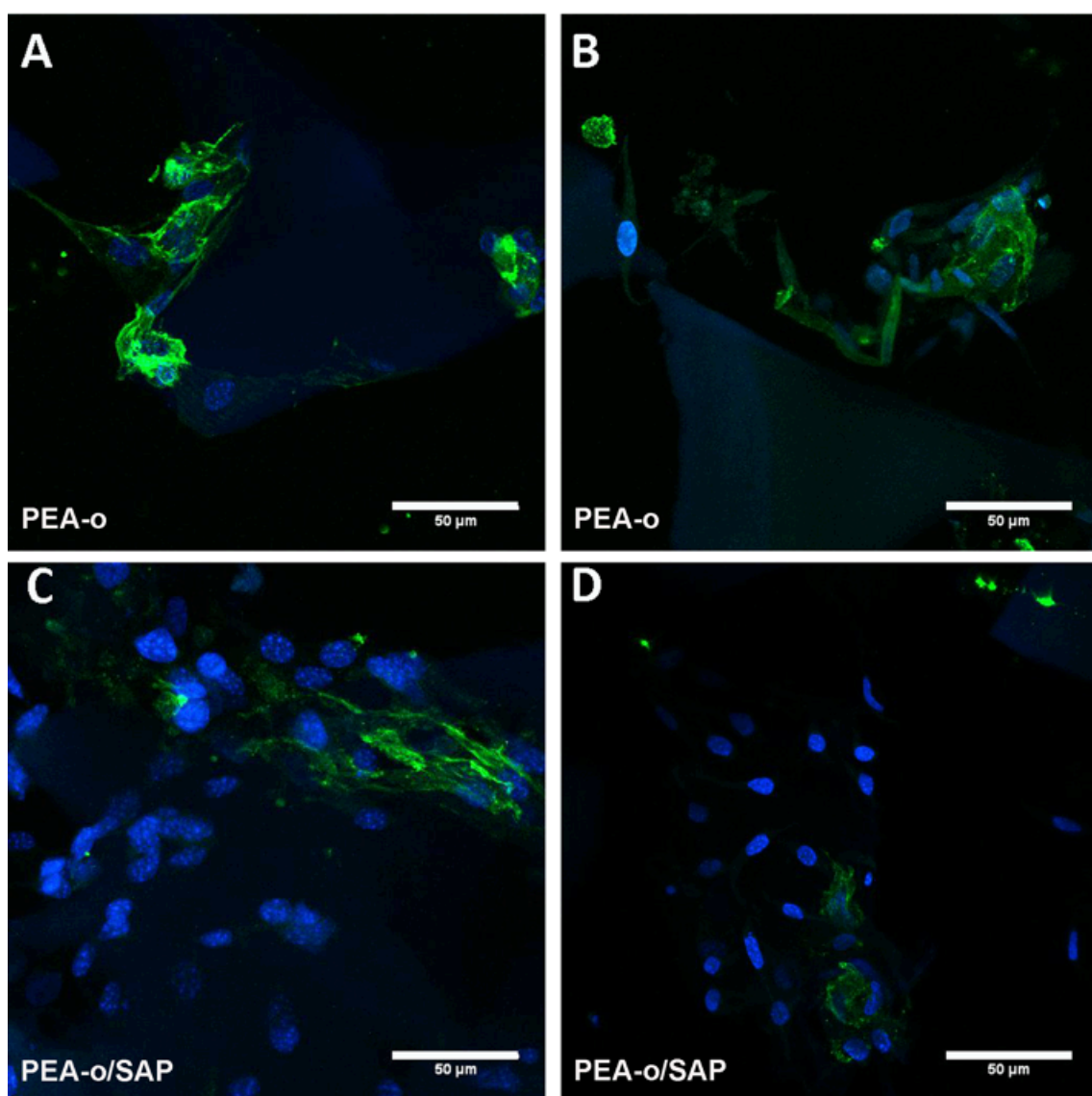
Figure 6: SEM images of the surface (A, C) and cross-sections (B, D) of PEA-s scaffolds without (A, B) and with SAP gel in their pores (C, D), seeded dynamically with HUVECs and hADSCs, after 10 days of culture. Insets show details of regions of interest at greater magnification.

Figure 7: CLSM images of the surface (A, C) and cross-sections (B, D) of HUVECs/hADSCSs co-cultures stained against CD31 (green) and DAPI (blue) in bare PEA-o scaffolds (A, B) and with SAP gel (C, D). After 10 days of culture the cell density in the PEA-o scaffolds was scarce, either with (C, D) or without SAP gel in the pores (A, B).
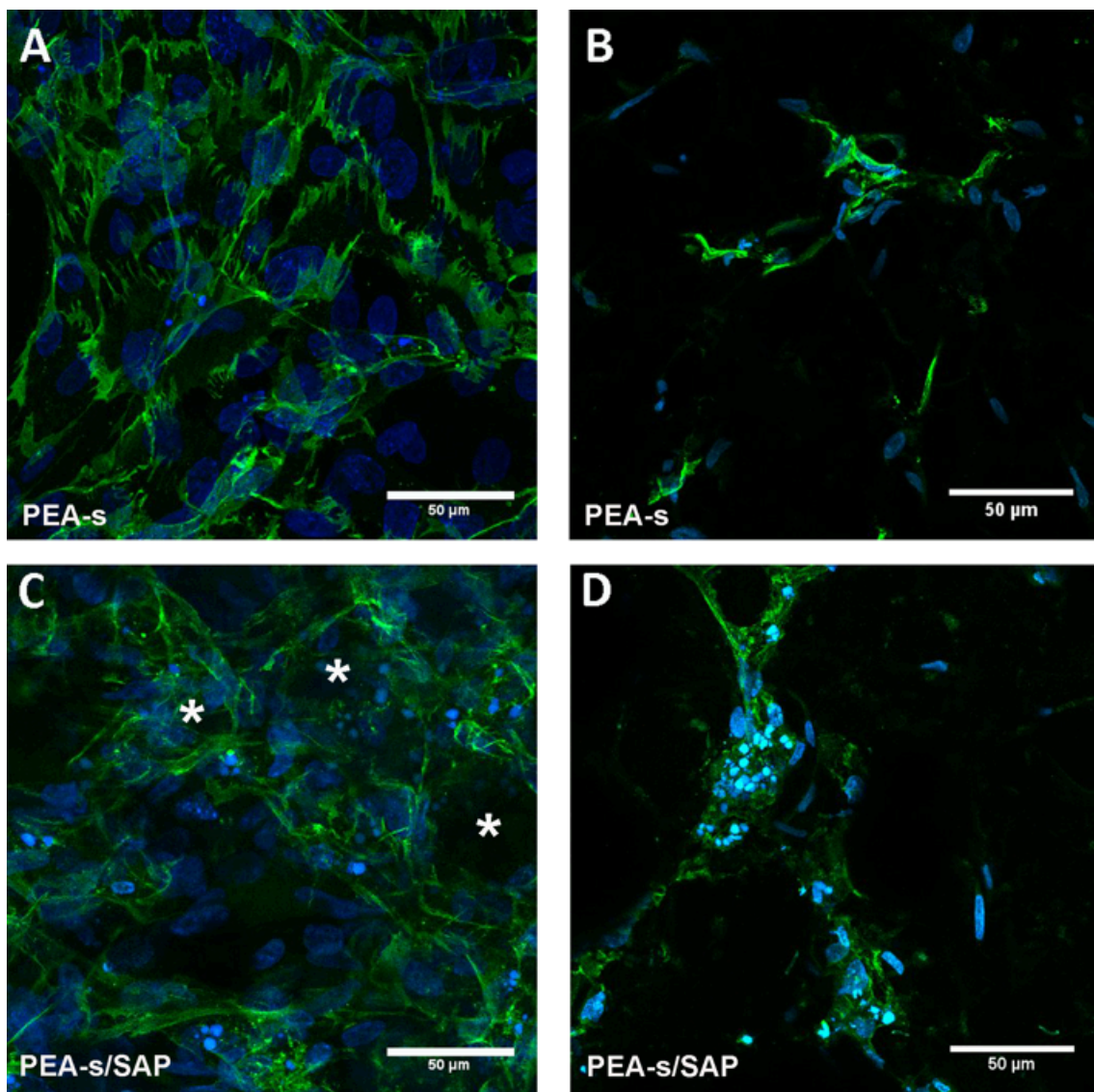
Figure 8: CLSM images of the surface (A, C) and cross-sections (B, D) of HUVECs/hADSCSs co-cultures stained against CD31 (green) and DAPI (blue), in bare PEA-s scaffolds (A, B) and with SAP gel (C, D). After 10 days of culture, cells show an optimal growth in PEA scaffolds with spherical pores (A, B) and a number of cell-cell connections in scaffolds with SAP (asterisks in C).
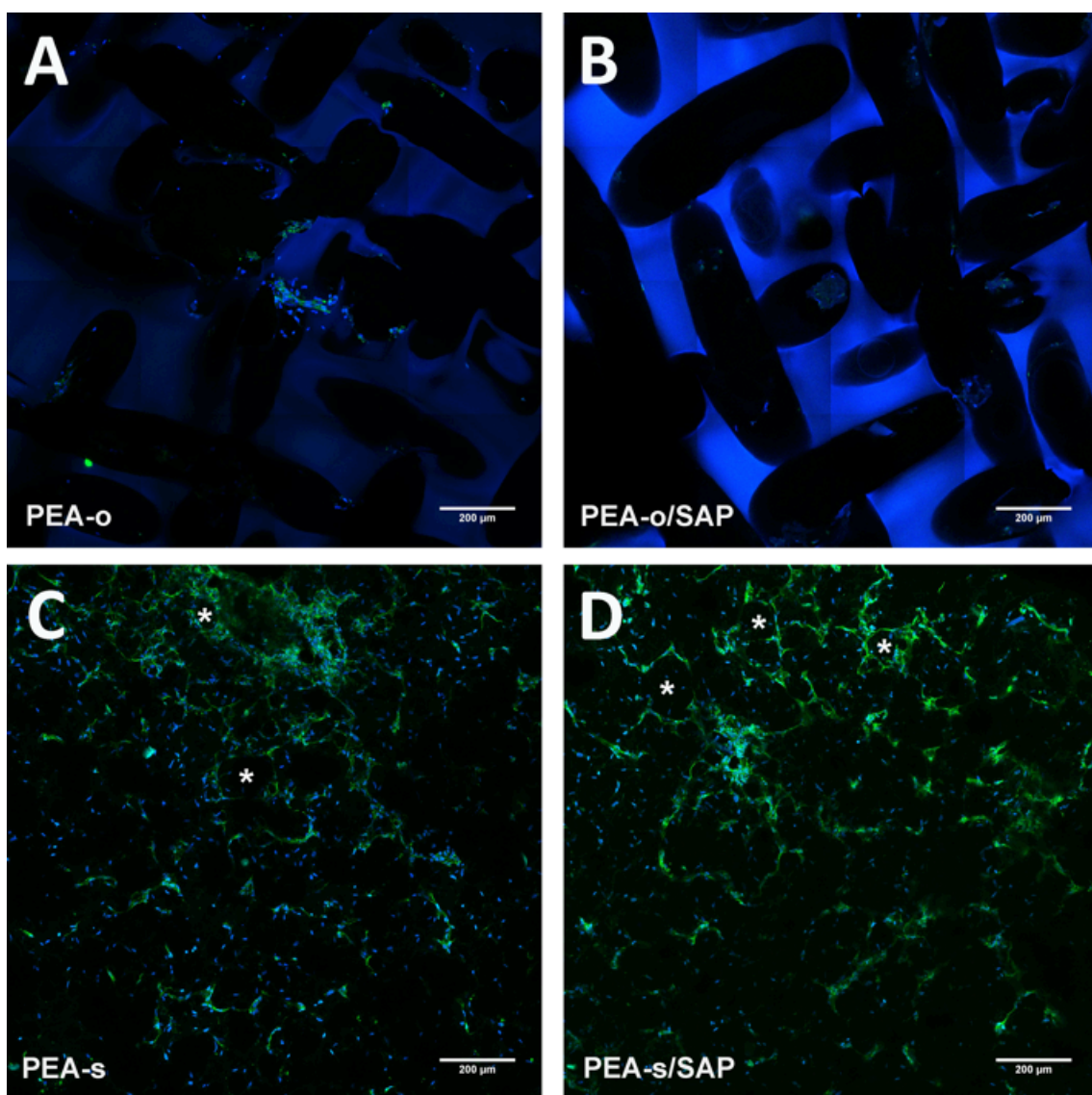
Figure 9: CLSM overview images (16 images per group) of inner sections of bare (left) and SAP-filled (A, B) PEA-o (C, D), and PEA-s scaffolds (second row) cultured with HUVECs/hADSCSs for 10 days. DAPI staining for nuclei (blue) and CD31 positive cells for endothelial cells (green).
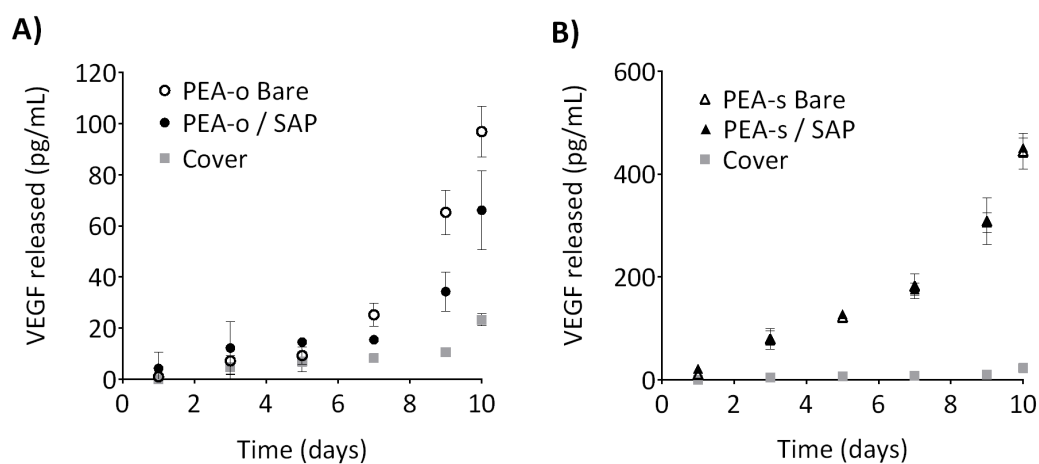
Figure 10: Cumulative VEGF released to the culture medium by cells cultured in PEA-o (A) and PEA-s (B) scaffolds compared with release from cultures on coverslips. Note the different scales of the ordinate axis in both figures. Statistically significant differences were found between PEA-o bare samples and PEA-s ones and between PEA-o gel-filled samples and PEA-s counterparts.